Agricultural and Forest Meteorology 345 (2024) 109850

Contents lists available at ScienceDirect

Agricultural and Forest Meteorology

journal homepage: www.elsevier.com/locate/agrformet

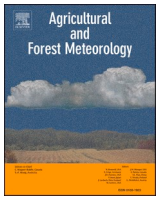

Site matters - Canopy conductance regulation in mature temperate trees diverges at two sites with contrasting soil water availability

David N. Steger [a,b,c,d,*], Richard L. Peters [b,e,1], Theresa Blume [f], Alexander G. Hurley [a], Daniel Balanzategui [a,g], Daniel F. Balting [a,h], Ingo Heinrich [a,c,d]

[a] GFZ German Research Centre for Geosciences, Section Climate Dynamics and Landscape Evolution, Telegrafenberg, 14473 Potsdam, Germany
[b] University of Basel, Department of Environmental Sciences, Physiological Plant Ecology Group, Schönbeinstrasse 6, 4056 Basel, Switzerland
[c] Humboldt-Universität zu Berlin, Geography Department, Climate Geography, Unter den Linden 6, 10099 Berlin, Germany
[d] DAI Deutsches Archäologisches Institut, Podbielskiallee 69-71, 14195 Berlin, Germany
[e] Laboratory of Plant Ecology, Department of Plants and Crops, Faculty of Bioscience Engineering, Ghent University, Coupure links 653, B-9000 Ghent, Belgium
[f] GFZ German Research Centre for Geosciences, Section Hydrology, Telegrafenberg, 14473 Potsdam, Germany
[g] Technical University of Applied Sciences Lübeck, Mönkhofer Weg 239, 23562 Lübeck, Germany
[h] Alfred Wegener Institute, Helmholtz Centre for Polar and Marine Research, Bussestr. 24, 27570 Bremerhaven, Germany

ARTICLE INFO

Keywords:
Canopy conductance
European forest
Soil drought
Sap flow
Dendrometer
Intraspecific variability
Water-use strategy
Adjustment
Tree water supply and demand

ABSTRACT

Tree-specific canopy conductance (G_c) and its adjustment play a critical role in mitigating excess water loss in changing environmental conditions. However, the change of G_c sensitivity to environmental conditions due to drought remains unclear for European tree species. Here we quantified the environmental operational space of G_c, i.e., the water supply (soil moisture, tree water deficit) and demand conditions (vapor pressure deficit) under which $G_c \geq 50\%$ is possible (G_{c50}OS), at two sites with different soil water availability for three common European tree species. We collected sap flow and dendrometer measurements for co-occurring *Pinus sylvestris, Fagus sylvatica* and *Quercus petraea* growing under different soil hydrological conditions (drier/wetter). These measurements were combined with meteorological variables and soil moisture conditions in five depths. Dendrometer measurements were used to confirm soil water availability patterns. For all analyses, the contrasting soil hydrology between sites was the main driver of G_c response. At the drier sites, *F. sylvatica* and *P. sylvestris* reduced their water consumption in response to decreasing soil water supply earlier in the growing season than *Q. petraea*. However, our analysis on the G_{c50}OS revealed that at the drier sites, *F. sylvatica* and *Q. petraea* reduced the extent of their G_{c50}OS to a higher degree than *P. sylvestris*. This indicates a higher level of G_{c50}OS adjustment to the drier site conditions for the two broadleaved species. These differences were more pronounced when using the dendrometer-derived tree internal water status as proxy for tree water supply. Our results provide preliminary evidence for diverging short-term G_c responses when temperate trees are exposed to prolonged reduction in water availability. These findings suggest that G_{c50}OS can help to constrain species-specific predictions of water use by mature trees, especially when combined with high-resolution water potential measurements.

1. Introduction

Recent observations and climate projections show persistent increases in vapor pressure deficit (*D*), soil drought, and extreme drought event frequency for temperate regions (Dai 2013; Grossiord et al., 2020; Balting et al., 2021; Satoh et al., 2022; Nagavciuc et al., 2023). These negatively impact forest ecosystems by reducing tree-internal water status and detrimentally altering leaf phenology, which can lead to declining stem growth and higher tree mortality rates (Babst et al., 2019; Arend et al., 2022; Li et al., 2022; Hammond et al., 2022; Salomón et al., 2022; Wu et al., 2022). A commonly known strategy for trees to mitigate the adverse effects of drought is to reduce water loss through the leaves by stomatal closure (Damour et al., 2010; Buckley, 2019). The regulation of stomatal closure and its impact on water conductance through

* Corresponding author.
E-mail address: david.steger@unibas.ch (D.N. Steger).
[1] Equally contributing first author.

https://doi.org/10.1016/j.agrformet.2023.109850
Received 10 August 2023; Received in revised form 26 October 2023; Accepted 1 December 2023
Available online 11 December 2023

the tree canopy can be expressed as whole-tree canopy conductance (G_c; e.g., Pappas et al., 2018; Peters et al., 2019). Understanding the mechanisms driving G_c is crucial for explaining drought resistance of trees, but also for improving predictions on the global hydrological cycle (Schlesinger and Jasechko 2014; Mastrotheodoros et al., 2020). Furthermore, changes of G_c regulation as response to water scarcity could impact the trees' water-use efficiency and thus have wide-ranging implications for the linkage between water and carbon cycle, productivity and species composition of forests (e.g., Mastrotheodoros et al., 2017; Fatichi et al., 2022). Therefore, it is valuable to examine G_c and its response of mature trees to water supply and demand in relation to drought vulnerability (Martinez-Vilalta et al., 2019; Carminati and Javaux 2020; Flo et al., 2021; Joshi et al., 2022).

Adjustment, including acclimation and modification, can be considered an adapted physiological response that allows trees to maintain homeostasis during long-term environmental change (e.g., Larcher 2003). This can lead to within species variability of physiological climate responses when comparing, for example, wet and dry habitats (Domec et al., 2009; Marchin et al., 2016). During periods of short-term increase in *D,* G_c shows a non-linear decrease towards full stomatal closure (Oren et al., 1999; Grossiord et al., 2020; Flo et al. 2022). This response could, however, change to some extent due to adjustment to long-term drier conditions (e.g., Marchin et al., 2016). Observations on forest-level conductance from flux tower measurements revealed that forest sites in drier habitats indeed show a stronger stomatal down-regulation with increasing *D* when soil moisture is lower (Novick et al., 2016). However, when moving to the tree species-specific level, adjustment of stomatal regulation appears more complex (e.g., Mencuccini 2003; Beikircher and Mayr 2009; Marchin et al., 2016; Limousin et al., 2022), with some coniferous tree species showing lower G_c with increasing *D* under experimentally induced drier conditions (Grossiord et al., 2017), while species like *Pinus sylvestris* seemed to be less affected by changes in long-term water availability (Poyatos et al., 2007; Schönbeck et al. 2022). For broadleaved tree species, a wide variability in water-use-climate responses was found, with ring-porous species such as *Quercus petraea* at persistently drier sites showing almost no change in stem sap flow dynamics to *D* (which are driven by G_c) compared to more diffuse-porous species like *Fagus sylvatica* (e.g., Bader et al., 2022; Fabiani et al., 2023). Comparing intraspecific variability in G_c-climate responses under persistently different site conditions avoids the temporally limited scope of manipulation experiments (Tomasella et al., 2017, Grossiord et al., 2018) and thus may provide important insights into species adjustment to changed environments (Novick et al., 2016). However, other confounding factors besides drought, such as tree architecture (Mencuccini 2003) and soil properties (Hacke et al., 2000) could impact G_c response (i.e., a common challenge for this space-for-time approach; Pickett 1989)."

Quantifying shifts in the down-regulation of G_c to drought due to adjustment poses several challenges. First, *D* and soil water availability (also expressed as relative extractable water, REW) simultaneously impact G_c sensitivity (Fu et al., 2022), where the response to both environmental drivers could change due to G_c adjustment. To avoid collinearity issues, analyses often isolate subjectively selected soil moisture classes and assess the response slope of the decrease in G_c due to increasing *D* in accordance with Eq. (1) (Oren et al., 1999; Novick et al., 2016; Bachofen et al., 2023):

$$G_c = -m \cdot ln(D) + b \quad (1)$$

where the parameter *m* quantifies the relative sensitivity of G_c to *D*, and b is the reference conductance at $D = 1$. Here, some studies focus on the adjustment of the slope (*m* or sensitivity parameter; e.g., Pappas et al., 2018; Peters et al., 2019; Schönbeck *et al.* 2022), while other studies discuss changes in both parameters (e.g., Poyatos et al., 2007; Marchin et al., 2016; Flo et al., 2021), making interpretations of maximum G_c changes versus relative changes in a non-linear response slope to *D* difficult. As such, some studies instead focus on the environmental or physiological conditions (e.g., leaf water potential) at which 50% of maximum stomatal conductance is reached, as these provide simpler indicators for environmental constraints on stomatal operation (Klein 2014; Anderegg et al., 2017). A second challenge is that soil water availability is heavily dependent upon general rooting depths and the observed potential to temporally lower root-water uptake depth during drought (Brinkmann et al., 2018a; Kahmen et al., 2021, 2022). More critically, soil moisture measurements at multiple soil depths are difficult to obtain (but see Walthert et al., 2021), and assessing the spatio-temporal changes in soil water availability is complex (Brinkmann et al., 2018a,b). Therefore, instead of measuring soil moisture, studies begin to utilize internal tree-water status, obtained directly from leaf water potential measurements which however are more labor-intensive (Klein 2014; Steppe 2018), or indirectly with automated stem dendrometer measurements (Dietrich et al., 2019; Salomón et al., 2022). A promising approach would thus be to explore the environmental conditions that constrain G_c operation, where a shift in those conditions, as consequence of persistent exposure to wetter or drier habitats (i.e., different soil water availability), indicates adjustment of G_c regulation. Accordingly, we defined the operational space of canopy conductance as the water supply (REW, tree water deficit) and demand (*D*) conditions under which $G_c \geq 50\%$ of its maximum is possible (G_{c50}OS).

This work presents a case-study on the adjustment potential of G_{c50}OS of three mature tree species growing at two sites with contrasting soil water availability, i.e., wetter and drier, in a temperate forest. We collected and analyzed sap flow and dendrometer data from the same trees of the three main temperate forest species *Pinus sylvestris, Fagus sylvatica*, and *Quercus petraea* for the period from 2012 to 2019. For each species, we investigated trees growing at two neighboring sites characterized by persistent differences in soil water availability (drier/wetter) for a study period long enough to provide observations covering similar environmental conditions (*D*, REW) in short-term variability between sites. Due to their spatial proximity (max. 50 m distance, Fig. 1), trees experienced similar *D* conditions while exposed to long-term differences in soil water availability (considered as drier and wetter habitats), due to well-drained sandy soils and topography at the study site. Soil moisture was measured from 10 to 70 cm depth. The patterns of soil water availability were related to pre-dawn minimum tree water deficit to confirm the responsiveness of the trees to soil water availability in particular measurements depths. As broadleaved tree species generally are known to have a more rapid and active stomatal control (Brodribb et al., 2017), we expect to find more adjustment to drier habitats of the G_{c50}OS expressed in a stronger down-regulation of G_c at the drier site for *F. sylvatica* and *Q. petraea*, while finding little adjustment for *P. sylvestris* (Schönbeck et al., 2022).

2. Materials and methods

2.1. Study site and monitoring design

The study site is located in the Müritz National Park (53.33 °N, 13.19 °E) within the TERENO Observatory in the lowlands of northeastern Germany (TERENO-NE; Fig. 1a). Müritz National Park provides near-natural conditions representative for temperate lowland mixed forests (Heinrich et al., 2018). The glacially-formed landscape features a mosaic of lakes and terminal moraines, with elevations ranging from 63 m above sea level at lake level to 125 m a.s.l.. The resulting highly variable ground-water table depths and the high permeability of the sandy soils together create a diverse range of hydrological regimes over relatively small distances (see Heinrich et al., 2018 for a detailed site description). The climate is temperate with a mean annual temperature of 8.8 °C and relatively dry with annual precipitation of 591 mm over the period 1981-2010 (DWD, 2023).

A total of 22 mature trees were monitored from 2012 until 2019, covering *Pinus sylvestris* L., *Fagus sylvatica* L., and *Quercus petraea* Liebl..

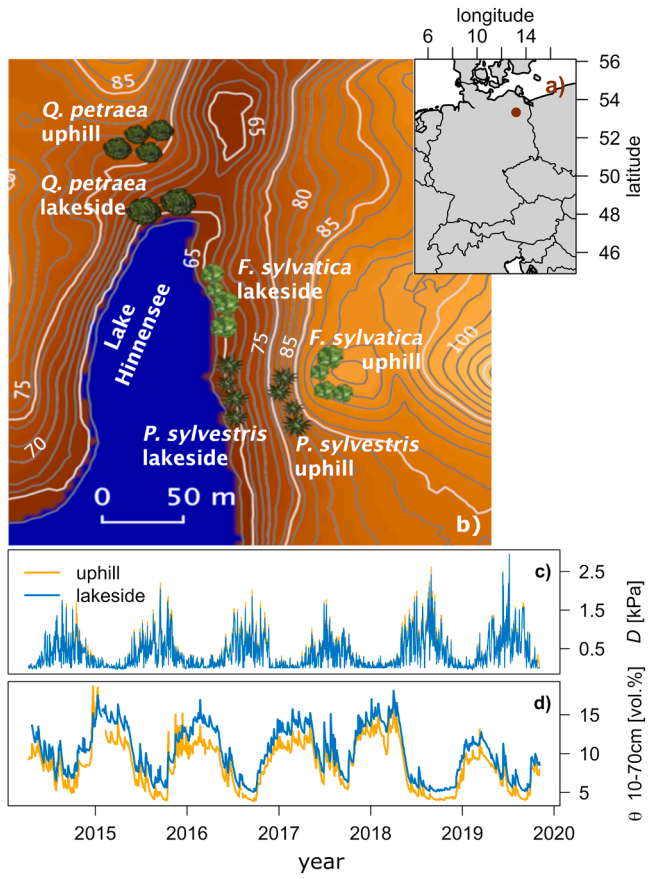

Fig. 1. Study site and environmental conditions. a) The location of the TERENO—NE Hinnensee monitoring site, with a sketch of the experimental design of the study site and b) arrangement of individual tree monitoring sites, namely uphill and lakeside. The lines are elevation contours. c) Mean time-series (n = 6) of vapor pressure deficit (D), and d) soil moisture (θ, averaged across 10–70 cm depth) dynamics at the two sites, highlighting the consistently drier soil conditions at the uphill site for the period 2014–2019.

At each site, only healthy dominant or co-dominant trees growing closely together were selected (see Siegmund et al., 2016) which resulted in an average replication of four individuals per species and site (Table 1). For each tree, sub-hourly sap flow and dendrometer measurements were collected, with concurrent climate and soil moisture measurements at each site, to assess canopy conductance (G_c; see Table A.1 for used abbreviations and symbols) dynamics and the tree-internal water status. For each tree, multiple allometric characteristics were determined (Table 1), including diameter at breast height (d_{stem}), tree height (h_{tree}) and crown height (h_c; using a Vertex IV, Haglöf, Sweden), sapwood thickness (t_{sw}; visually detected from the collected tree cores), maximum bark (t_{ba}; measured at the four cardinal directions, including phloem and cork), and phloem thickness (t_{phl}; measured from the tree cores). For each species, trees were selected which were exposed to either drier or wetter soil water availability conditions, while standing close enough together to experience similar atmospheric conditions. The first set of species-specific monitoring sites is located close to lake Hinnensee (Fig. 1b; hence referred to as lakeside site). The second group of monitoring sites is located along a moraine saddle and slope (Fig. 1b; hence referred to as uphill site). Indeed, the two contrasting sites showed almost identical vapor pressure deficit conditions (D; Fig. 1c), while the lakeside sites experienced wetter soil moisture conditions compared to the uphill site, due to their proximity to a shallow groundwater table (Fig. 1d).

2.2. Environmental measurements

At each monitoring site, atmospheric and soil moisture conditions have been monitored since 2014. Air temperature (T_a in °C), relative humidity (RH in%), and volumetric soil moisture (θ in vol.%) were continuously recorded at a 10-minute interval using a Campbell Scientific CR1000 data logger (Campbell Scientific Inc., Logan, USA). T_a and RH were measured in 2 m above ground and recorded using Campbell Scientific CS215 sensors. D (in kPa) was calculated from T_a and RH by using the R package *plantecophys* (Duursma, 2015). These measurements were complemented with hourly radiation data (in W m^{-2}) and precipitation measurements (in mm), as well as T_a and RH data from 2012 to 2014, measured by a nearby climate station (*Messstation Serrahn*; < 5 km distance). θ was measured with Truebner SMT100 sensors (Truebner GmbH, Neustadt, Germany), where at each individual tree monitoring site these sensors were installed at 10, 20, 30, 50, and 70 cm depth with a minimal replication of three sensors per depth. To present a normalized and comparable measure of plant-available soil water between uphill and lakeside sites, we calculated the relative extractable water (REW) from θ at each tree monitoring site, and depth combination according to Eq. (2). Here, θ_{max} is the 95th percentile of θ and θ_{min} is the absolute minimum for each sensor.

$$REW = \frac{\theta - \theta_{min}}{\theta_{max} - \theta_{min}} \quad (2)$$

θ_{max} and θ_{min} of all sensors were in the range of values for field capacity and permanent wilting point reported by Saxton & Rawls (2006) and for values derived from pedotransfer functions for sandy forest soils (e.g., Teepe et al., 2003). To represent the soil water status (soil water availability), we calculated the mean REW over all measured depths for all subsequent analyses. All environmental measurements were averaged to hourly values, as this was the minimum temporal resolution of the nearby climate station.

2.3. Sap flow monitoring and canopy conductance calculation

Each monitored tree was instrumented with Granier type sap flow sensors (Granier, 1987), installed at 1.3 m height on the tree stem. The sensors consisted of two standard thermal dissipation probes and two reference probes, with the latter being used to correct for natural thermal drift in the stem temperature (SF-L sensors, Ecomatik, Munich, Germany). Each probe contains a thermocouple that measures sapwood temperature along a 20 mm long needle, installed according to the manufacturer's specifications. For trees with sapwood depth < 20 mm, a Clearwater correction (Clearwater et al., 1999) was applied to account for probe sections that were installed in non-conducting heartwood (Table 1, OUP1). Temperature differences between the probes (ΔT) were measured at a 30-minute interval and stored on a CR800 data logger (Campbell Scientific Inc., Logan, USA). The ΔT measurements obtained from sap flow sensors were inspected and outliers were removed using the R package *datacleanr* (Hurley et al., 2022). The cleaned ΔT measurements were converted to sap flux density (F_d; kg m^{-2} s^{-1}) using the TREX R package (Peters et al., 2021), while applying i) the double-regression method to establish zero-flow conditions (using a 5-day period), ii) sapwood corrections (using t_{sw} of *QP_UP1* in Table 1), and iii) species- (*F. sylvatica*) or wood-specific (*P. sylvestris* = Coniferous, and *Q. petraea* = Ring-porous) calibrations (as calibration studies were not present for all species). During the study period, several sap flow sensors were re-installed at different sides of the trees. However, to account for dampening effects in the sap flow measurements (Peters et al., 2018) and to make the sap flow measurements comparable among trees and sensors, F_d values were rescaled for each individual tree and year to the 95th percentile that was reached in 2012 – the vegetation period after the first installation of all sensors (assuming a tree reaches maximum transpiration rates in each year; see Peters et al., 2018).

Table 1
Characteristics of trees instrumented for continuous monitoring. For each tree growing at a specific site, diameter at breast height (d_{stem}), tree height (h_{tree}), crown height (h_c), sapwood thickness (t_{sw}), maximum bark thickness (t_{ba}), and phloem thickness (t_{phl}) were measured. Tree codes: *PS = Pinus sylvestris, FS = Fagus sylvatica, QP = Quercus petraea, UP* = uphill, *LA* = lakeside.

site	species	tree	d_{stem} [cm]	h_{tree} [m]	h_c [m]	t_{sw} [cm]	t_{ba} [cm]	t_{phl} [mm]
uphill	***Pinus sylvestris***	*PS_UP1*	51.9	26.5	9.6	8.8	3.0	4.0
		PS_UP2	52.1	23.2	7.4	6.6	3.3	1.5
		PS_UP3	59.3	27.4	10.0	8.1	3.5	1.0
		PS_UP4	60.2	24.0	7.7	6.6	4.8	2.0
		mean	**55.9**	**25.3**	**8.7**	**7.5**	**3.6**	**2.1**
	Fagus sylvatica	*FS_UP1*	40.1	18.5	14.0	9.8	0.9	6.0
		FS_UP2	40.1	17.9	9.4	8.4	1.1	7.0
		FS_UP3	33.1	17.9	10.0	6.8	0.9	5.0
		FS_UP4	36.6	17.4	8.3	7.9	1.0	6.0
		mean	**37.5**	**17.9**	**10.4**	**8.2**	**0.9**	**6.0**
	Quercus petraea	*QP_UP1*	65.9	29.4	13.2	2.0	1.8	4.0
		QP_UP2	68.1	31.8	9.8	1.4	2.6	5.0
		QP_UP3	71.4	36.3	14.3	2.1	2.4	4.0
		QP_UP4	89.6	35.1	14.6	4.4	3.3	6.0
		mean	**73.8**	**33.2**	**13.0**	**2.5**	**2.5**	**4.8**
lakeside	***Pinus sylvestris***	*PS_LA1*	63.6	31.8	8.2	7.5	3.9	1.0
		PS_LA2	50.9	26.5	5.4	6.5	4.1	1.5
		PS_LA3	48.1	22.5	3.9	4.8	3.4	1.0
		PS_LA4	64.3	32.7	8.4	7.0	3.7	2.0
		mean	**56.7**	**28.4**	**6.5**	**6.5**	**3.8**	**1.4**
	Fagus sylvatica	*FS_LA1*	42.2	25.6	12.7	13.7	1.0	5.0
		FS_LA2	67.2	21.8	16.1	17.0	1.4	6.0
		FS_LA3	51.0	25.9	14.5	10.6	1.1	6.0
		FS_LA4	56.8	34.0	19.6	17.6	1.0	5.0
		mean	**54.3**	**26.8**	**15.7**	**14.7**	**1.1**	**5.5**
	Quercus petraea	*QP_LA1*	105.6	34.0	29.5	2.8	2.7	9.0
		QP_LA2	67.9	33.9	27.5	2.4	3.5	6.0
		mean	**86.8**	**33.9**	**28.5**	**2.6**	**3.1**	**7.5**

Whole-tree canopy conductance (G_c in mol m^{-2} s^{-1}) was calculated per unit sapwood area, as there were no accurate estimations available of the total leaf area per tree. G_c was calculated according to Flo et al. (2021; see Eq. (3)). We transformed the data to solar time and used the mean midday values (3 h before and after solar noon) for G_c calculation to reduce the impact of stem capacitance and delayed flow dynamics (see Pappas et al., 2018; Peters et al., 2019). Midday F_d, D, and T_a were used, in combination T_0 which is 273 K and h (m a.s.l.) which is the elevation of the site. Finally, η was used which is a constant equal to 44.6 mol m^{-3} and results from unit transformation on the approach by Phillips and Oren (1998) to calculate G_c (Flo et al., 2021). Midday mean G_c values were removed where $D < 0.5$ kPa and daily precipitation $>$ 0.5 mm d^{-1}. Moreover, we excluded days with midday values of global irradiance $<$ 400 W $m^{-2}h^{-1}$ and $T_a < 12$°C to isolate optimal transpiration conditions (see Peters et al., 2019).

$$G_c = \frac{(115.8 + 0.4236T_a)F_d}{D} \cdot n \cdot \frac{T_0}{(T_0 + T_a)} \cdot e^{-0.00012 \cdot h} \quad (3)$$

2.4. Dendrometer measurements and processing

For each monitored tree, stem radius variations (Δr_{stem} in µm) were recorded using high-resolution point dendrometers (DR Radius Dendrometer, Ecomatik, Munich, Germany). The dendrometers were installed at the same height and opposite to the sap flow sensors and recorded Δr_{stem} with a 30-minute resolution. Δr_{stem} was processed to partition growth (i.e., irreversible radius increments) and water-related components (i.e., reversible stem shrinkage and expansion) using the *treenetproc* R package (Knüsel et al., 2021). This partitioning is performed according to the commonly used zero-growth concept (Zweifel et al., 2016), where radius variations below the preceding maximum stem radius are considered as periods of tree water deficit (TWD in µm; i.e., a more severe stem shrinkage results in higher TWD; see Fig. 2) - a proxy for the internal water status of the tree (Dietrich et al., 2018; Salomón et al., 2022). TWD can be described as a measure of water loss from non-conducting stem tissue that occurs when transpiration exceeds root water uptake causing stems to shrink proportionally to the dehydration of elastic storage tissue (Dietrich et al., 2018).

During midday, TWD increases due to the transpiration of the tree, while during the night, TWD decreases and is mainly dependent upon the potential of the tree to rehydrate (e.g., Steppe et al., 2006; Peters et al., 2023). In most cases, daily minimum TWD is reached just before sunrise, and as such, represents the pre-dawn TWD conditions (Salomón et al., 2022). However, to isolate the rehydration status of the tree stem, we quantified minimum TWD only for pre-dawn conditions (abs. $TWD_{pd.min}$). As abs. $TWD_{pd.min}$ is affected by both the elasticity of the bark tissue and size of the tree, we normalized abs. $TWD_{pd.min}$ by dividing by the tree-specific maximum daily shrinkage of the entire time series (MDS; calculated as the 99th percentile of absolute daily shrinkage values across the monitoring period; Knüsel et al., 2021) to account for differences in absolute shrinkage potentials between trees ($TWD_{pd.min}$, resulting unit = µm µm^{-1}; see Fig. 2). Here it is assumed, that this diurnal radial shrinkage of the bark reflects the tree-specific differences in storage tissue flexibility and size. TWD values were constrained to the months June to September, representing the period with generally highest atmospheric demand and lowest soil water supply as well as least phenological variation. Moreover, this selection avoids winter-time shrinkage and phloem collapse patterns. As soil moisture measurements began in 2014, all subsequent response analyses reflect the period between June to September from 2014 to 2019.

2.5. Analyses of the operational space of canopy conductance

We define the operational space of canopy conductance in general (G_cOS) as a two-dimensional G_c response area shaped by water demand (D) and water supply, where water supply can be approached by soil water availability (REW) or by the internal water status of a tree ($TWD_{pd.min}$; if there are no leaf water potential measurements available). Thus, the G_cOS presents the range of environmental conditions at which canopy conductance in general is possible. To assess G_cOS, we

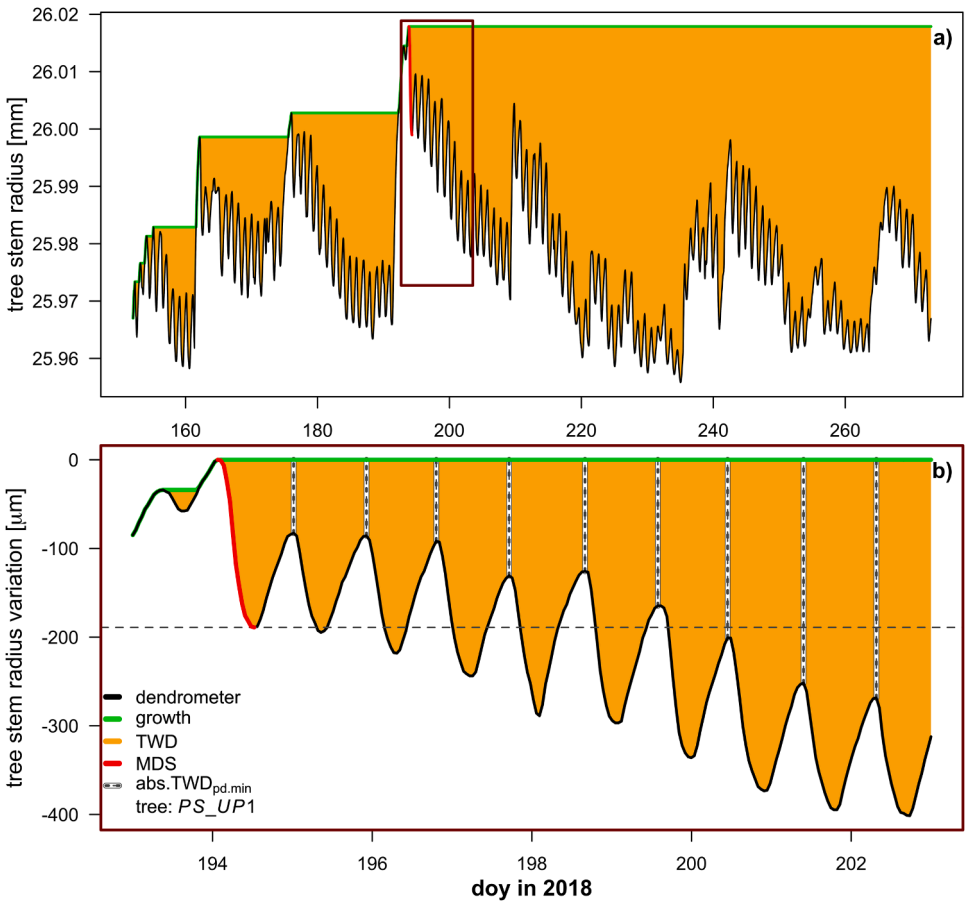

Fig. 2. Graphical depiction of dendrometer data and derivations of growth, tree water deficit (TWD), maximum daily shrinkage (MDS), and absolute pre-dawn minimum tree water deficit (abs. $TWD_{pd.min}$) as proxy for the stem water status of a tree. a) Time-series of the dendrometer against day of year (doy) for *PS_UP*1 (see Table 1), covering June to September 2018. b) A 10-day window of the dendrometer series presented in a). Until doy 194, the tree grew and afterwards the tree was not able to rehydrate fully during the night, which is illustrated by negative stem radius variations (increasing TWD; orange area). The maximum daily shrinkage (MDS = 99th percentile of absolute daily shrinkage) recorded for the tree is highlighted with a red line. Starting from doy 200, this tree showed $TWD_{pd.min}$ values above 1, as it exceeded the MDS (dotted line).

established inter- and intraspecific comparability by normalizing G_c values for each monitored tree by division with their 99th percentiles ($G_{c.norm}$). As G_c was calculated per sapwood area, $G_{c.norm}$ provides a unitless representation of the G_c regulation per sapwood area thus reducing the influence of tree architecture. We applied mixed effect models to derive $G_{c.norm}$ responses to *D* and REW ($G_{c.norm}$-*d*-REW) as well

Table 2
Overview of models with model structures with $G_{c.norm}$ = normalized midday canopy conductance per unit sapwood area, $TWD_{pd.min}$ = pre-dawn minimum tree water deficit standardized by the maximum daily shrinkage, *D* = vapor pressure deficit, REW = relative extractable water, int = modelled intercepts, *a and b* = modelled slope parameters, RSE = relative standard error as ratio of the standard error to the corresponding model parameter, and $G_{c50}OS/G_cOS$ = ratio of operational space of canopy conductance (G_cOS) at $G_c \geq 50\%$ ($G_{c50}OS$) to the G_cOS with common environmental conditions.

model	structure	site	species	int	RSE_{int} [0–1]	p_{int}	*a*	RSE_a [0–1]	p_a	*b*	RSE_b [0–1]	p_b	$\frac{G_{c50}OS}{G_cOS}$ [0–1]
$G_{c.norm}$–*D*-*REW*	$\sqrt{G_{c.norm}} = \frac{a}{\sqrt{D}} + b*log(REW)$	**uphill**	***P. sylvestris***	0.44	0.08	<0.001	0.57	0.04	<0.001	0.52	0.02	<0.001	0.38
			F. sylvatica	0.51	0.06	<0.001	0.47	0.04	<0.001	0.44	0.02	<0.001	0.39
	random effects		***Q. petraea***	0.11	0.34	0.006	0.66	0.04	<0.001	0.18	0.05	<0.001	0.27
	individual trees:	**lakeside**	***P. sylvestris***	0.26	0.09	<0.001	0.59	0.02	<0.001	0.25	0.03	<0.001	0.35
	random intercepts		***F. sylvatica***	0.38	0.11	<0.001	0.42	0.06	<0.001	0.11	0.15	<0.001	0.44
			Q. petraea	0.11	0.28	0.001	0.58	0.04	<0.001	−0.03	0.41	0.017	0.37
$G_{c.norm}$–*D*-$TWD_{pd.min}$	$\sqrt{G_{c.norm}} = \frac{a}{\sqrt{D}} + b*\sqrt{TWD_{pd.min}}$	**uphill**	***P. sylvestris***	0.50	0.09	<0.001	0.47	0.05	<0.001	−0.44	0.03	<0.001	0.42
			F. sylvatica	0.51	0.09	<0.001	0.36	0.07	<0.001	−0.51	0.03	<0.001	0.12
	random effects		***Q. petraea***	0.13	0.40	0.020	0.61	0.06	<0.001	−0.22	0.08	<0.001	0.18
	individual trees:	**lakeside**	***P. sylvestris***	0.21	0.20	0.001	0.58	0.03	<0.001	−0.17	0.06	<0.001	0.33
	random intercepts		***F. sylvatica***	0.39	0.14	<0.001	0.38	0.07	<0.001	−0.15	0.29	0.001	0.30
			Q. petraea	0.16	0.22	<0.001	0.55	0.05	<0.001	0.00	3.03	0.742	0.37

as to D and $TWD_{pd.min}$ ($G_{c.norm}$-d-$TWD_{pd.min}$). For each model, individual trees were treated as random effects (slopes and intercept), which provided us with four candidate models (no random effects, slope and intercept, slope only, intercept only). We used the Akaike information criterion (AIC) to select the final model (see Table 2 for model structures and parameters). In all cases, the best fitting model included the random effects of individual trees on the intercept, but no random effect on the explanatory variables, i.e., no random slopes (Table 2). We examined all assumptions for each model fit, including normality, heteroscedasticity, and independence, and applied variable transformations where necessary (Zuur et al., 2010).

To assess whether species adjust their G_cOS, we derived G_cOS with ≥ 50% of maximum G_c activity (G_{c50}OS) within a set of common environmental conditions (D, REW, and $TWD_{pd.min}$ values that were observed at all individual tree monitoring sites). The common environmental space allows for intra- and interspecific comparability. As adjustment can result in both G_c-environment response slopes as well as the magnitude of canopy conductance (Marchin et al., 2016) we address both parameters as follows: we refer to the steepness of the $G_{c.norm}$ response slopes to changes in a certain parameter as sensitivity, while we use the term down-regulation as a measure of inter- or intraspecific "absolute" difference between $G_{c.norm}$ values when comparing model responses and G_{c50}OS extents. For example, down-regulation was defined as the%-reduction of G_{c50}OS when comparing the uphill and lakeside sites with common conditions compared to%-reduction with dry soils (REW ≤ 0.2; Fig. 4). The final shapes of the G_{c50}OS were defined by i) the common environmental conditions (outer borders of grey area in Figs. 4a and 5), and ii) by the slope of the respective response model (shape of G_{c50}OS inside common conditions area). We quantified the extent of the response areas as bin count to establish comparability between G_{c50}OS (bin size = 0.002, i.e., model prediction for all possible combinations of D with REW or with $TWD_{pd.min}$ in steps of 0.002; see Table 2 and Table A.3 for absolute bin counts). Ratios describing the ratio of G_{c50}OS to the common G_cOS can be found in Table 2. All models, p-value determination, and model slope fixed effect tests for significant differences (see SI for fixed effect test description, Table A.4) were calculated using the *lmerTest* R package (Kuznetsova et al., 2017). Marginal mean significances between responses were calculated with the *emmeans* R package (Lenth 2023). A p-value ≤ 0.05 was considered statistically significant for all analyses. All model analyses were performed in R Studio (R Studio Team, 2020) using the R software version 3.6 (R Core Team, 2019).

3. Results

3.1. Species-specific sap flux density dynamics

Comparison of sap flux density (F_d) variability between uphill and lakeside sites revealed differences in water consumption per unit sapwood area, i.e., F_d (see Appendix, Fig. A.1 for time series of F_d per species). Overall, maximum hourly and daily F_d values were highest for *F. sylvatica* followed *by Q. petraea*, and lowest for *P. sylvestris* at both uphill and lakeside (Table A.2). Almost the same pattern was found for mean hourly and daily F_d, while lakeside *Q. petraea* showed lowest values. In general, highest F_d values, especially maximum F_d, were found for *F. sylvatica*, followed by *Q. petraea*, and *P. sylvestris*.

Seasonal dynamics of the mean normalized sap flux density per unit sapwood area ($F_{d.norm}$) revealed site-specific temporal patterns on water consumption (Fig. 3). Water consumption ($F_{d.norm}$) at the uphill sites was highest in May (*P. sylvestris*, $F_{d.norm}$ = 0.83) and June (*F. sylvatica* = 0.86; *Q. petraea* = 0.77) and decreased during the summer months for all species. At the wetter lakeside, the water consumption of all species stayed higher and more stable during the study period while gradually decreasing for *P. sylvestris* and *F. sylvatica* (Fig. 3). While at the beginning of the study period (June) $F_{d.norm}$ uphill and lakeside were similar per species (< 5% difference), in September, $F_{d.norm}$ at the uphill sites was lower by 22.5% for *F. sylvatica*, by 20.9% for *P. sylvestris*, and by 17.2% for *Q. petraea*.

3.2. Canopy conductance response to environmental drivers

The G_c-d-REW analysis revealed site-specific differences in $G_{c.norm}$

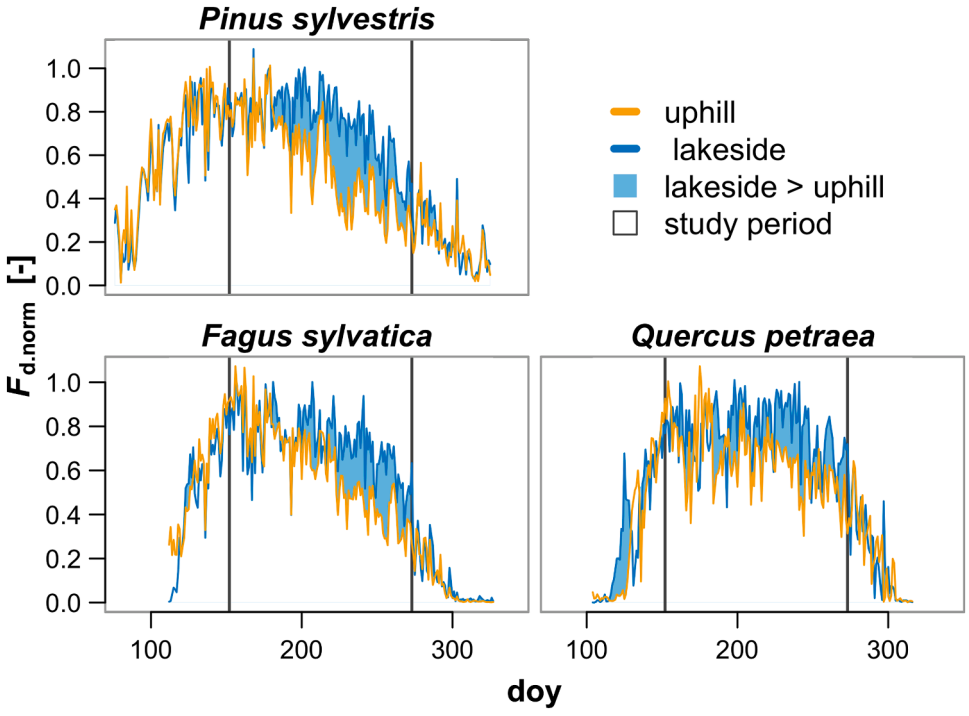

Fig. 3. Seasonal dynamics of the normalized midday sap flux density per sapwood area ($F_{d.norm}$) for each species illustrated as mean values per day of year (doy) over the period 2014 – 2019.

response slopes (*sensitivity*) towards changes in soil water supply (REW) where all species showed steeper $G_{c.norm}$ response slopes to decreasing REW at the drier uphill site with significant differences between sites and species. In contrast, there was no significant influence of the site to the species-specific $G_{c.norm}$ response to D (see Table A.4 for significances in slope differences and Fig. A.2 for a three-dimensional depiction of the G_c-d-REW analysis). *Q. petraea* displayed the steepest $G_{c.norm}$ response slope to D at the uphill site ($a = 0.66$) while at the lakeside, *Q. petraea* ($a = 0.58$) and *P. sylvestris* ($a = 0.59$) showed an equally steep $G_{c.norm}$ response to D (Table 2). *P. sylvestris* was most sensitive in its $G_{c.norm}$ response to REW ($b = 0.52$ [uphill]; $b = 0.25$ [lakeside]) compared to the other species (Table 2).

3.3. Operational space of canopy conductance

Regarding the operational space of canopy conductance with $G_c \geq 50\%$ (G_{c50}OS, common conditions: REW = [0, 0.7]; D = [0.5, 2.2] kPa), *F. sylvatica* showed higher G_c in a wider environmental space (defined by D and REW) than the other species, illustrated by the G_{c50}OS being larger in Fig. 4a (G_{c50}OS/G_cOS common = 0.39 uphill and 0.44 at lakeside). *P. sylvestris* showed the smallest differences in G_{c50}OS extents between sites with a 7.7% larger G_{c50}OS at the drier uphill site. *F. sylvatica* and *Q. petraea* showed smaller G_{c50}OS at the uphill sites (*F. sylvatica* = −12.1%, *Q. petraea* = −26.6%; see Table A.3 for absolute extents of G_cOS and G_{c50}OS). When comparing down-regulation of G_{c50}OS with situations of REW ≤ 0.2 (very dry soils, vertical line in Fig. 4a), *F. sylvatica* and *Q. petraea* showed a 15.8% reduction of the G_{c50}OS compared to *P. sylvestris* with 8.9% indicating a higher level of G_{c50}OS adjustment to drier conditions for *F. sylvatica* and *Q. petraea*. All p-values for slopes and intercepts were significant with $p \leq 0.02$ and relative standard errors were ≤ 0.2 (Table 2) indicating distinct $G_{c.norm}$ model responses to both REW and D. The absolute differences between the $G_{c.norm}$ response slopes to changes in D in situations with REW = 0.2 (G_c-D_{REW20}, Fig. 4b; see Table A.5 for marginal means) were not significant. For very dry (REW = 0.1) and very wet soils (REW = 0.6) all absolute G_c-D differences were significant except for *Q. petraea* at wet soils.

3.4. Canopy conductance response to vapor pressure deficit and tree water deficit

The $G_{c.nom}$-d-$TWD_{pd.min}$ analysis provided additional information of

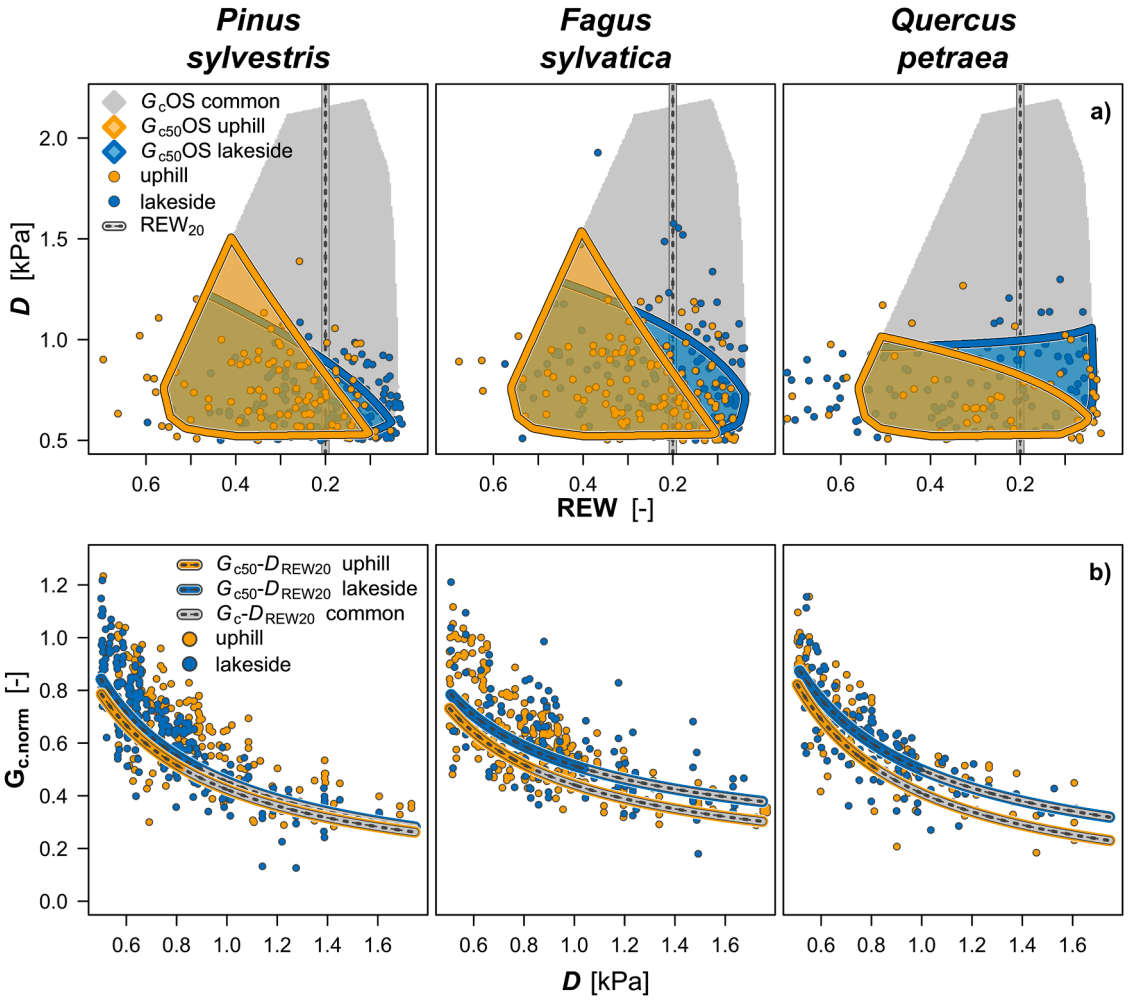

Fig. 4. Graphical depiction of $G_{c.norm}$-d-REW model results. a) operational space of canopy conductance (G_cOS) represented by the species-specific response area of canopy conductance ($G_{c.norm}$) to atmospheric evaporative demand (D) and relative extractable water (REW) with *grey area:* G_cOS for common environmental conditions (D and REW)*; colored areas:* G_cOS with $G_{c.norm} \geq 50\%$ of its maximum (G_{c50}OS); *dots*: original data points where $G_{c.norm} \geq 50\%$ of its maximum; *line*: line of relatively dry soil with 20% relative extractable water (REW_{20}). The borders of the G_{c50}OS that coincide with the grey area are defined by the common environmental conditions; the borders within the grey area are shaped by the modelled $G_{c.norm}$-d-REW response slope; b) shows a response of $G_{c.norm}$ to D along the REW_{20} line illustrated in panel a) (G_c-D_{REW20}). The colors indicate the site and the color-filled lines represent the part of the response with $G_{c.norm} \geq 50\%$ as illustrated in panel a) (G_{c50}-D_{REW20}).

G_c regulation towards water demand and supply particularly for *F. sylvatica*. The patterns of $G_{c.norm}$ sensitivity to D were similar to the $G_{c.nom}$-d-REW analysis for all species. $G_{c.nom}$ response slopes to $TWD_{pd.min}$ were steepest for *F. sylvatica* at the uphill site, whereas at lakeside its response was equally sensitive to that of *P. sylvestris* (Table 2). All species showed significant intraspecific differences in their $G_{c.norm}$ response slopes to D and $TWD_{pd.min}$.

Within common conditions of atmospheric demand (D = [0.5, 2.2] kPa) and stem shrinkage ($TWD_{pd.min}$ = [0, 0.7] μm μm^{-1}), $G_{c50}OS$ was largest for *P. sylvestris* ($G_{c50}OS/G_cOS = 0.42$) at the uphill site and at the lakeside it was largest for *Q. petraea* ($G_{c50}OS/G_cOS = 0.37$) while it was lowest for *F. sylvatica* at both sites (Table 2). The patterns of $G_{c50}OS$ variability between sites were comparable to the G_c-d-REW analysis (Fig. 5). However, the differences were pronounced for $G_{c.nom}$-d-$TWD_{pd.min}$ where *P. sylvestris* showed a higher $G_{c50}OS$ by 26.2% at the uphill site while *F. sylvatica* showed a reduction in $G_{c50}OS$ by 59.8% and *Q. petraea* by 53.0% (Fig. 5). Except for *Q. petraea,* which showed a non-significant $G_{c.norm}$ response to $TWD_{pd.min}$, all p-values for slopes and intercepts were significant with $p \leq 0.001$ (Table 2).

4. Discussion

We found differing extents of the environmental space at which >50% of canopy conductance (G_c) is sustained, which we refer to as the operational space of canopy conductance ($G_{c50}OS$). We can clearly relate this extent to the contrasting soil water availability across sites which the studied tree species were exposed to. Our results show that mature *P. sylvestris, F. sylvatica* and *Q. petraea* down-regulate G_c more to increasing D and show higher G_c sensitivity to decreasing water availability when comparing the drier with the wetter site. Although this is consistent with general findings on the forest-stand level (e.g., Novick et al., 2016, Bachofen et al., 2023), our case-study shows that the $G_{c50}OS$ appears to adjust differently between *P. sylvestris, F. sylvatica and Q. petraea*. Although longer-term drier conditions are likely to increase periods of stomatal closure, we find that the impact of reduced water availability on forest transpiration might be highly dependent upon the future species composition and the range of environmental variability. Yet, to fully confirm these findings we would require high-resolution and long-term measurements of leaf water potential as an additional and more direct indicator of the tree water status (Steppe 2018; Peters et al., 2023).

4.1. Higher adjustment of canopy conductance for Fagus sylvatica and Quercus petraea

F. sylvatica and *Q. petraea* showed larger shifts in the operational space of canopy conductance when comparing wetter with drier habitats at the study site, with uphill $G_{c50}OS$ (drier habitat) for *F. sylvatica* being smaller by 46.8% and for *Q. petraea* by 48.2% compared to the lakeside $G_{c50}OS$ (wetter habitat) when considering REW ≤ 0.3 (Fig. 4). The smaller difference in $G_{c50}OS$ extents for *P. sylvestris* compared to *F. sylvatica* and *Q. petraea* (Fig. 4a) matches well with multiple studies which found little adjustment for *P. sylvestris* in its stomatal response to D with decreasing soil water availability (e.g., Poyatos et al., 2007; Schönbeck et al., 2022). However, while Bader et al. (2022) did not report significant changes for *Q. petraea* in its G_c response to D with lower soil water availability in wetter or drier habitats, our results did show an adjustment of the $G_{c50}OS$ (Fig. 4a). This discrepancy could be explained by soil properties, as the soils studied by Bader et al. (2022) were not as well drained as the sandy soils at our study site and sandy soils are suspected to generally increase G_c-D sensitivity (Cai et al., 2022). Moreover, Fabiani et al. (2023) found significant differences in water-use of *F. sylvatica* growing on a hilltop (drier) and at footslope (wetter) indicating adjustment in water-use driven by soil water availability. In

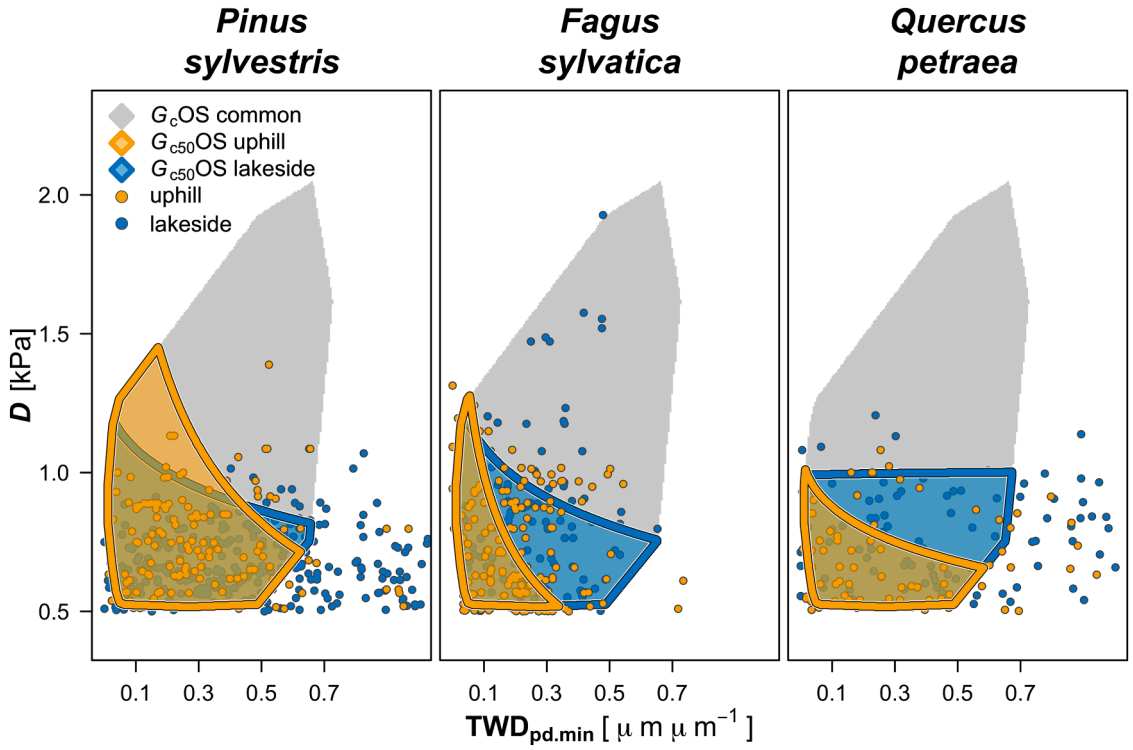

Fig. 5. Graphical depiction of operational space of canopy conductance (G_cOS) with *grey area* = G_cOS for common atmospheric and tree water status conditions (vapor pressure deficit D and minimum pre-dawn tree water deficit $TWD_{pd.min}$); *colored areas:* G_cOS with $G_{c.norm} \geq 50\%$ of its maximum ($G_{c50}OS$); *dots*: original data points where $G_{c.norm} \geq 50\%$. The borders of the $G_{c50}OS$ that coincide with the grey area are defined by the common environmental conditions (D and $TWD_{pd.min}$) which were chosen for intra- and interspecific comparability reasons as well as the comparability with the $G_{c.norm}$-d-REW findings illustrated in Figure 4a; the borders within the grey area are shaped by the modelled $G_{c.norm}$-d-$TWD_{pd.min}$ response slope.

addition, Denham et al. (2020) found decreasing soil moisture to be driving G_c-*D* sensitivity for oak species in the USA. Our finding on the adjustment potential of *Q. petraea* also seems to match better with the relatively high variability in the leaf water potentials at which 50% of stomatal conductance is reached for ring-porous species (Klein 2014). However, at the southernmost distribution limit of *F. sylvatica* and *Q. petraea, F. sylvatica* appeared to be slightly more sensitive to increasing *D* (Aranda et al., 2000), which for our study is only the case when the REW is extremely low (REW $\leq$ 0.1 in Fig. 4a; in contrast to Bader et al., 2022). These results illustrate that we cannot with certainty state whether either *F. sylvatica* or *Q. petraea* is more capable of adjusting their G_{c50}OS to drier habitats, as G_c adjustment seems to strongly depend on the range of soil moisture levels which the trees have experienced and how this subsequently affects the internal water status of the individual tree.

The adjustment of the G_c-environment response to drier habitats and conditions can involve physiological, anatomical, or morphological changes in trees to improve performance or survival (Larcher 2003; Demmig-Adams et al., 2008). One possible reason for the interspecific difference in G_{c50}OS adjustment can be found in the evolution of stomatal regulation: while species such as *F. sylvatica* and *Q. petraea* developed a more rapid abscisic acid (ABA) pathway which allows for active stomatal regulation, conifers such as *P. sylvestris* rely on passive processes (Brodribb et al., 2017). Higher active stomatal regulation of *Q. petraea* and *F. sylvatica* compared to *P. sylvestris* is also suggested by the finding that broadleaved species in general can change stomatal regulation to CO_2 more than conifers (Klein and Ramon 2019). Wood anatomical reasons for the higher adjustment of *Q. petraea* and *F. sylvatica* include the higher potential to adjust the hydraulic conductivity of the sapwood of ring-porous and diffuse-porous wood structures compared to tracheid-bearing *P. sylvestris* (Zimmermann and Tyree 2002; Steppe and Lemeur, 2007; Zimmermann et al., 2021). Morphological traits regarding adjustment include the balance between root distribution versus total leaf area, which impacts soil water uptake depth and subsequently stomatal control (Carminati and Javaux 2020; Kahmen et al. 2022) which might be one more explanation for the observed difference in G_{c50}OS adjustment.

4.2. Adjustment to vapor pressure deficit at the drier site

Large emphasis has been put on understanding stomatal or G_c response and its adjustment potential to *D* during droughts (e.g., Marchin et al., 2016; Grossiord et al., 2017, 2020; Flo et al., 2021, 2022; Martín-Gómez et al., 2023). However, when a tree is exposed to a dry habitat (i.e., with more frequent occurrences of low REW), it stands to reason that when the drought is absent, the tree takes full advantage of the improved water availability due the limited assimilation potential across the growing season (McDowell et al., 2008; as found for temperature adjustment; Marchin et al., 2016; Peters et al., 2019; Fabiani et al., 2023). This expected shift to a water-spending water-use strategy at the drier habitats when REW is not low (i.e., REW > 0.3 in Fig. 4a) is hinted at by our case-study, where G_{c50}OS is larger at higher REW for uphill (drier habitat) *F. sylvatica* (+12%) and *P. sylvestris* (+21.4%; Fig. 4a) compared to the lakeside trees (wetter habitat). Although we need to consider that various traits influence the importance of this relative G_c adjustment for the individual (e.g., total leaf area, sapwood-to-leaf area; Mencuccini et al., 2019), higher $G_{c.norm}$ in response to *D* during wet periods could potentially offset some of the drought-induced assimilation losses for *P. sylvestris* and *F. sylvatica* (Fig. 4). This can be supported by the significant differences in marginal means of the G_c-*D* responses with high REW (0.6) for the two species (Table A.4) as well as their gradual reduction of water consumption at the uphill sites during the study period (Fig. 3; see also Fabiani et al., 2023). These findings raise the question why the lakeside trees down-regulated G_c and G_{c50}OS more strictly to increasing *D* and thus reduced relative assimilation rates in situations with higher REW (Fig. 4a).

The reduced G_c down-regulation with increasing *D* and wetter soils (REW > 0.3) at the drier uphill site disappeared for *F. sylvatica* when considering tree water deficit as water supply for the determination of G_{c50}OS, while *P. sylvestris* still showed a similar increase in G_{c50}OS with equivalently little stem shrinkage (expressed as $TWD_{pd.min}$; Fig. 5). Using stem shrinkage instead of REW has the advantage of approaching the drought stress of a tree closer than by using soil moisture (Dietrich et al., 2018; Salomón et al., 2022). Moreover, using $TWD_{pd.min}$ as proxy for tree water supply provides an additional insight into the potential shifts that could have made the G_{c50}OS response of *F. sylvatica* and *P. sylvestris* possible at wetter conditions (Fig. 4a). For *F. sylvatica* the increased G_{c50}OS adjustment during wetter conditions (REW > 0.3), but not with similar shrinkage (Fig. 5), could be explained by the ability of the uphill trees to shift their root water uptake depth more than the trees at the lakeside as the higher water table might prevent the lakeside trees from rooting deeper (Brinkmann et al., 2018a). This can be supported by Fabiani et al. (2023) reporting a lighter xylem water isotopic composition of *F. sylvatica* growing on a footslope (wetter) indicating less use of seasonal water sources due to closer connectivity to groundwater sources compared to hilltop trees (drier). *F. sylvatica* and *Q. petraea* could also benefit more from hydraulic lift than *P. sylvestris* (as discussed by Bader et al., 2022), as their vessels allow for greater hydraulic conductivity than tracheids (Tyree and Zimmermann 2002; Aranda et al., 2005). The adjustment of consistently increased G_{c50}OS with both wetter conditions and higher tree-internal water availability for *P. sylvestris* is likely caused by higher capacitance of stored water within the flexible tissues for trees growing at the uphill site (e.g., Zweifel et al., 2005; Verbeeck et al., 2007; Salomón et al., 2017). Also, *P. sylvestris* is considered a species that is already adapted to a wide range of (often very dry) habitats (Poyatos et al., 2007) and thus likely is not impacted by the drier site conditions at the uphill site, which might explain why we could not find the same level of adjustment as for *F. sylvatica* and *Q. petraea*. In addition, of the studied species, *P. sylvestris* potentially has the highest difficulties of night-time rehydration (Peters et al., 2023). This could explain the lack of a G_{c50}OS increase at the wetter site as the trees might not be able to fully benefit from more available water. Although further research is required to determine the exact water status of the trees and the mechanism underlying the G_{c50}OS adjustment, our findings highlight the species-specific nature of G_c adjustment to drier habitats.

5. Conclusions

Our analyses of the operational space of canopy conductance (G_{c50}OS) highlight its adjustment potential in species like *P. sylvestris, F. sylvatica* and *Q. petraea*. Our case-study demonstrates that, when comparing drier and wetter site conditions, *F. sylvatica* and *Q. petraea* are able to adjust their G_{c50}OS to drier habitats more than *P. sylvestris*. This suggests that within temperate forests of comparable species composition, transpiration rates of the studies species (as G_c is closely linked to transpiration; Hernandez-Santana et al., 2016) might decrease more during droughts in case a habitat becomes persistently drier, forcing trees to reduce G_c sensitivity to *D* during wetter periods. This might also affect the local timing of transpiration and might have unknown impacts on forest stand transpiration and its modelling (e.g., Schlesinger and Jasechko 2014; Mastrotheodoros et al., 2020).

Our simplified approach of quantifying the environmental and physiological space at which $\geq$ 50% of maximum G_c is possible, appears promising in supporting the identification of water-use strategies and provides insights in adjustment dynamics of whole-tree canopy conductance of the studied species in response to drought. Moreover, incorporating point dendrometer measurements to derive stem-water status as proxy for tree water availability is highly promising in deriving the G_{c50}OS. In addition, using leaf water potential measurements would be critical to directly assess the tree-water status to

determine tree water-use strategies and their adjustment. As we focused on three common European tree species growing in one temperate forest, applying this approach to more sites of different stand densities, climates and environments as well as studying further species, might mark a promising step in enhancing our understanding of the G_c and G_{c50}OS adjustment potential of mature trees to a drier and hotter future.

Supporting data and information

Additional supporting information and data may be found online in the Supporting information section at the end of the article.

Funding

RLP acknowledges the support of the Swiss National Science Foundation (SNSF), Grant P2BSP3_184475. DFB is funded by the PalEX Project (AWI Strategy Fund). AGH was supported through the Helmholtz-Climate-Initiative (HI-CAM), funded by the Helmholtz Initiative and Networking Fund.

Authors' contributions

DNS and RLP designed the study. TB, DB, DFB, and IH provided necessary data. IH and TB managed the TERENO—NE project and experimental design of the research site. Discussions among all authors contributed to the conceptual development of this study. DNS and RLP wrote the initial manuscript with aid from IH, to which all authors contributed revisions.

Declaration of Competing Interest

The authors declare that they have no known competing financial interests or personal relationships that could have appeared to influence the work reported in this paper.

Data availability

Data will be made available on request.

Acknowledgements

We thank Markus Morgner and Jörg Wummel for technical support and maintenance of the study site. We thank Christoforos Pappas and Christoph Schneider for their support and discussion. Furthermore, we would like to thank the Müritz National Park authorities for their support. This study has used infrastructure of the Terrestrial Environmental Observatory (TERENO – Northeast), of the Helmholtz Association. The authors are responsible for the content of this publication.

Supplementary materials

Supplementary material associated with this article can be found, in the online version, at doi:10.1016/j.agrformet.2023.109850.

References

Anderegg, W.R.L., Wolf, A., Arango-Velez, A., Choat, B., Chmura, D.J., Jansen, S., Kolb, T., Li, S., Meinzer, F., Pita, P., Resco de Dios, V., Sperry, J.S., Wolfe, B.T., Pacala, S., 2017. Plant water potential improves prediction of empirical stomatal models. PLoS ONE 12 e0185481–e0185481. https://pubmed.ncbi.nlm.nih.gov/29023453.

Aranda, I., Gil, L., Pardos, J.A., 2000. Water relations and gas exchange in Fagus sylvatica L. and Quercus petraea (Mattuschka) Liebl. in a mixed stand at their southern limit of distribution in Europe. Trees 14, 344–352. https://doi.org/10.1007/s004680050229.

Aranda, I., Gil, L., Pardos, J.A., 2005. Seasonal changes in apparent hydraulic conductance and their implications for water use of European beech (Fagus sylvatica L.) and sessile oak [Quercus petraea (Matt.) Liebl] in South Europe. Plant Ecol. 179, 155–167. https://doi.org/10.1007/s11258-004-7007-1.

Arend, M., Link, R.M., Zahnd, C., Hoch, G., Schuldt, B., Kahmen, A., 2022. Lack of hydraulic recovery as a cause of post-drought foliage reduction and canopy decline in European beech. New Phytol. 234, 1195–1205. https://doi.org/10.1111/nph.18065.

Babst, F., Bouriaud, O., Poulter, B., Trouet, V., Girardin, M.P., Frank, D.C., 2019. Twentieth century redistribution in climatic drivers of global tree growth. Sci. Adv. 5, eaat4313. https://doi.org/10.1126/sciadv.aat4313.

Bachofen, C., Poyatos, R., Flo, V., Martínez-Vilalta, J., Mencuccini, M., Granda, V., Grossiord, C., 2023. Stand structure of Central European forests matters more than climate for transpiration sensitivity to VPD. J. Appl. Ecol. 60, 886–897.

Bader, M.K.-F., Scherrer, D., Zweifel, R., Körner, C., 2022. Less pronounced drought responses in ring-porous than in diffuse-porous temperate tree species. Agric. For. Meteorol. 327, 109184. https://www.sciencedirect.com/science/article/pii/S0168192322003719.

Balting, D.F., AghaKouchak, A., Lohmann, G., Ionita, M., 2021. Northern Hemisphere drought risk in a warming climate. npj Clim. Atmos. Sci. 4, 61. https://doi.org/10.1038/s41612-021-00218-2.

Beikircher, B., Mayr, S., 2009. Intraspecific differences in drought tolerance and acclimation in hydraulics of Ligustrum vulgare and Viburnum lantana. Tree Physiol. 29, 765–775.

Brinkmann, N., Eugster, W., Buchmann, N., Kahmen, A., 2018a. Species-specific differences in water uptake depth of mature temperate trees vary with water availability in the soil. Plant Biol. 21.

Brinkmann, N., Seeger, S., Weiler, M., Buchmann, N., Eugster, W., Kahmen, A., 2018b. Employing stable isotopes to determine the residence times of soil water and the temporal origin of water taken up by Fagus sylvatica and Picea abies in a temperate forest. New Phytol. 219, 1300–1313. https://doi.org/10.1111/nph.15255.

Brodribb, T.J., McAdam, S.A.M., Carins Murphy, M.R., 2017. Xylem and stomata, coordinated through time and space. Plant Cell Environ. 40, 872–880. https://doi.org/10.1111/pce.12817.

Buckley, T.N., 2019. How do stomata respond to water status? New Phytol. 224, 21–36. https://doi.org/10.1111/nph.15899.

Cai, G., König, M., Carminati, A., Abdalla, M., Javaux, M., Wankmüller, F., Ahmed, M.A., 2022. Transpiration response to soil drying and vapor pressure deficit is soil texture specific. Plant Soil 1–17.

Carminati, A., Javaux, M., 2020. Soil Rather Than Xylem Vulnerability Controls Stomatal Response to Drought. Trends Plant Sci. 25, 868–880. https://doi.org/10.1016/j.tplants.2020.04.003.

Clearwater, M.J., Meinzer, F.C., Andrade, J.L., Goldstein, G., Holbrook, N.M., 1999. Potential errors in measurement of nonuniform sap flow using heat dissipation probes. Tree Physiol. 19, 681–687.

Dai, A., 2013. Increasing drought under global warming in observations and models. Nat. Clim. Chang. 3, 52–58. https://doi.org/10.1038/nclimate1633.

Damour, G., Simonneau, T., Cochard, H., Urban, L., 2010. An overview of models of stomatal conductance at the leaf level. Plant Cell Environ. 33, 1419–1438. https://doi.org/10.1111/j.1365-3040.2010.02181.x.

Demmig-Adams B., Dumlao M.R., Herzenach M.K., Adams W.W. (2008) Acclimation. In: Jørgensen SE, Fath BDBT-E of E (eds.) Academic Press, Oxford, pp 15–23. https://www.sciencedirect.com/science/article/pii/B978008045405400001X.

Denham, S.O., Oishi, A.C., Miniat, C.F., Wood, J.D., Yi, K., Benson, M.C., Novick, K.A., 2020. Eastern US deciduous tree species respond dissimilarly to declining soil moisture but similarly to rising evaporative demand. Tree Physiol. 41, 944–959.

Dietrich, L., Zweifel, R., Kahmen, A., 2018. Daily stem diameter variations can predict the canopy water status of mature temperate trees. Tree Physiol. 38, 941–952. https://doi.org/10.1093/treephys/tpy023.

Dietrich, L., Delzon, S., Hoch, G., Kahmen, A., 2019. No role for xylem embolism or carbohydrate shortage in temperate trees during the severe 2015 drought. J. Ecol. 107, 334–349. https://doi.org/10.1111/1365-2745.13051.

Domec, J.-C., Palmroth, S., Ward, E., Maier, C.A., Thérézien, M., Oren, R.A.M., 2009. Acclimation of leaf hydraulic conductance and stomatal conductance of Pinus taeda (loblolly pine) to long-term growth in elevated CO2 (free-air CO2 enrichment) and N-fertilization. Plant Cell Environ. 32, 1500–1512. https://doi.org/10.1111/j.1365-3040.2009.02014.x.

Duursma, R.A., 2015. Plantecophys - An R package for analysing and modelling leaf gas exchange data. PLoS One 10, 1–13. https://doi.org/10.1371/journal.pone.0143346.

DWD (German Weather Service), 2023. Wetter Und Klima aus Einer Hand. Wetter und Klima vor Ort: Waren. DWD, Offenbach, Germany. https://www.dwd.de/DE/wetter/wetterundklima_vorort/mecklenburg-vorpommern/waren/_node.html [accessed: 21 July 2023].

Fabiani, G., Klaus, J., Penna, D., 2023. Contrasting water use strategies of beech trees along two hillslopes with different slope and climate. Hydrol. Earth Syst. Sci. Discuss. 2023, 1–32.

Fatichi S., Pachalis A., Bonetti S., Manoli G. Pappas C. (2022) Water use efficiency: a review of spatial and temporal variability. update of Kirkham MB (2005) Encyclopedia of soils in the environment. Article Titles W:315–322. https://doi.org/10.1016/B0-12-348530-4/00441-0.

Flo, V., Martínez-Vilalta, J., Mencuccini, M., Granda, V., Anderegg, W.R.L., Poyatos, R., 2021. Climate and functional traits jointly mediate tree water-use strategies. New Phytol. 231, 617–630. https://doi.org/10.1111/nph.17404.

Flo, V., Martínez-Vilalta, J., Granda, V., Mencuccini, M., Poyatos, R., 2022. Vapour pressure deficit is the main driver of tree canopy conductance across biomes. Agric. For. Meteorol. 322, 109029.

Fu, Z., Ciais, P., Prentice, I.C., Gentine, P., Makowski, D., Bastos, A., Luo, X., Green, J.K., Stoy, P.C., Yang, H., Hajima, T., 2022. Atmospheric dryness reduces photosynthesis

along a large range of soil water deficits. Nat. Commun. 13, 989. https://doi.org/10.1038/s41467-022-28652-7.
Granier, A., 1987. Evaluation of transpiration in a Douglas-fir stand by means of sap flow measurements. Tree Physiol. 3, 309–320. https://doi.org/10.1093/treephys/3.4.309.
Grossiord, C., Sevanto, S., Borrego, I., Chan, A.M., Collins, A.D., Dickman, L.T., Hudson, P.J., McBranch, N., Michaletz, S.T., Pockman, W.T., Ryan, M., Vilagrosa, A., McDowell, N.G., 2017. Tree water dynamics in a drying and warming world. Plant Cell Environ. 40, 1861–1873. https://doi.org/10.1111/pce.12991.
Grossiord, C., Sevanto, S., Limousin, J.-M., Meir, P., Mencuccini, M., Pangle, R.E., Pockman, W.T., Salmon, Y., Zweifel, R., McDowell, N.G., 2018. Manipulative experiments demonstrate how long-term soil moisture changes alter controls of plant water use. Environ. Exp. Bot. 152, 19–27. https://www.sciencedirect.com/science/article/pii/S0098847217303301.
Grossiord, C., Buckley, T.N., Cernusak, L.A., Novick, K.A., Poulter, B., Siegwolf, R.T.W., Sperry, J.S., McDowell, N.G., 2020. Plant responses to rising vapor pressure deficit. New Phytol. 226, 1550–1566. https://doi.org/10.1111/nph.16485.
Hacke, U.G., Sperry, J.S., Ewers, B.E., Ellsworth, D.S., Schafer, K.V.R., Oren, R., 2000. Influence of soil porosity on water use in Pinus taeda. Oecologia 124, 495–505.
Hammond, W.M., Williams, A.P., Abatzoglou, J.T., Adams, H.D., Klein, T., López, R., Sáenz-Romero, C., Hartmann, H., Breshears, D.D., Allen, C.D., 2022. Global field observations of tree die-off reveal hotter-drought fingerprint for Earth's forests. Nat. Commun. 13, 1761. https://doi.org/10.1038/s41467-022-29289-2.
Heinrich, I., Balanzategui, D., Bens, O., Blasch, G., Blume, T., Böttcher, F., Borg, E., Brademann, B., Brauer, A., Conrad, C., Dietze, E., Dräger, N., Fiener, P., Gerke, H.H., Güntner, A., Heine, I., Helle, G., Herbrich, M., Harfenmeister, K., Heußner, K.U., Hohmann, C., Itzerott, S., Jurasinski, G., Kaiser, K., Kappler, C., Koebsch, F., Liebner, S., Lischeid, G., Merz, B., Missling, K.D., Morgner, M., Pinkerneil, S., Plessen, B., Raab, T., Ruhtz, T., Sachs, T., Sommer, M., Spengler, D., Stender, V., Stüve, P., Wilken, F., 2018. Interdisciplinary geo-ecological research across time scales in the northeast German Lowland observatory (TERENO-NE). Vadose Zone J. 17 https://doi.org/10.2136/vzj2018.06.0116.
Hernandez-Santana, V., Fernández, J.E., Rodriguez-Dominguez, C.M., Romero, R., Diaz-Espejo, A., 2016. The dynamics of radial sap flux density reflects changes in stomatal conductance in response to soil and air water deficit. Agric. For. Meteorol. 218-219, 92–101. https://www.sciencedirect.com/science/article/pii/S0168192315007649.
Hurley, A.G., Peters, R.L., Pappas, C., Steger, D.N., Heinrich, I., 2022. Addressing the need for interactive, efficient, and reproducible data processing in ecology with the datacleanr R package. PLoS One 17, e0268426. https://doi.org/10.1371/journal.pone.0268426.
Joshi, J., Stocker, B.D., Hofhansl, F., Zhou, S., Dieckmann, U., Prentice, I.C., 2022. Towards a unified theory of plant photosynthesis and hydraulics. Nat. Plants 8, 1304–1316. https://doi.org/10.1038/s41477-022-01244-5.
Kahmen, A., Buser, T., Hoch, G., Grun, G., Dietrich, L., 2021. Dynamic 2H irrigation pulse labelling reveals rapid infiltration and mixing of precipitation in the soil and species-specific water uptake depths of trees in a temperate forest. Ecohydrology 14, e2322. https://doi.org/10.1002/eco.2322.
Kahmen, A., Basler, D., Hoch, G., Link, R.M., Schuldt, B., Zahnd, C., Arend, M., 2022. Root water uptake depth determines the hydraulic vulnerability of temperate European tree species during the extreme 2018 drought. Plant Biol. 24, 1224–1239. https://doi.org/10.1111/plb.13476.
Klein, T., Ramon, U., 2019. Stomatal sensitivity to CO2 diverges between angiosperm and gymnosperm tree species. Funct. Ecol. 33, 1411–1424. https://doi.org/10.1111/1365-2435.13379.
Klein, T., 2014. The variability of stomatal sensitivity to leaf water potential across tree species indicates a continuum between isohydric and anisohydric behaviours. Funct. Ecol. 28, 1313–1320. https://doi.org/10.1111/1365-2435.12289.
Knüsel, S., Peters, R.L., Haeni, M., Wilhelm, M., Zweifel, R., 2021. Processing and extraction of seasonal tree physiological parameters from stem radius time series. Forests 12. https://www.mdpi.com/1999-4907/12/6/765.
Kuznetsova, A., Brockhoff, P.B., Christensen, R.H.B., 2017. lmerTest package: tests in linear mixed effects models. J. Stat. Softw. 82 https://doi.org/10.18637/jss.v082.i13.
Larcher, W., 2003. Physiological Plant Ecology: Ecophysiology and Stress Physiology of Functional Groups, 4th Edition. Springer, New York, p. 513. https://doi.org/10.1007/978-3-662-05214-3.
Lenth R. (2023). _emmeans: estimated Marginal Means, aka Least-Squares Means_. R package version 1.8.4-1, <https://CRAN.R-project.org/package=emmeans>.
Li, W., Migliavacca, M., Forkel, M., Denissen, J.M.C., Reichstein, M., Yang, H., Duveiller, G., Weber, U., Orth, R., 2022. Widespread increasing vegetation sensitivity to soil moisture. Nat. Commun. 13, 3959. https://doi.org/10.1038/s41467-022-31667-9.
Limousin, J., Roussel, A., Rodríguez-Calcerrada, J., Torres-Ruiz, J.M., Moreno, M., de Jalon, L.G., Ourcival, J., Simioni, G., Cochard, H., Martin-StPaul, N., 2022. Drought acclimation of Quercus ilex leaves improves tolerance to moderate drought but not resistance to severe water stress. Plant Cell Environ. 45, 1967–1984.
Marchin, R.M., Broadhead, A.A., Bostic, L.E., Dunn, R.R., Hoffmann, W.A., 2016. Stomatal acclimation to vapour pressure deficit doubles transpiration of small tree seedlings with warming. Plant Cell Environ. 39, 2221–2234. https://doi.org/10.1111/pce.12790.
Martín-Gómez, P., Rodríguez-Robles, U., Ogée, J., Wingate, L., Sancho-Knapik, D., Peguero-Pina, J., dos Silva, J.V.S., Gil-Pelegrín, E., Pemán, J., Ferrio, J.P., 2023. Contrasting stem water uptake and storage dynamics of water-saver and water-spender species during drought and recovery. Tree Physiol. 00, 1–17. https://doi.org/10.1093/treephys/tpad032.
Martinez-Vilalta, J., Anderegg, W.R.L., Sapes, G., Sala, A., 2019. Greater focus on water pools may improve our ability to understand and anticipate drought-induced mortality in plants. New Phytol. 223, 22–32. https://doi.org/10.1111/nph.15644.
Mastrotheodoros, T., Pappas, P.Molnar, Burlando, P., Keenan, T.F., Gentine, P., Gough, C.M., Fatichi, S., 2017. Linking plant functional trait plasticity and the large increase in forest water use efficiency. J. Geophys. Res. Biogeosci. 122, 2393–2408. https://doi.org/10.1002/2017JG003890.
Mastrotheodoros, T., Pappas, C., Molnar, P., Burlando, P., Manoli, G., Parajka, J., Rigon, R., Szeles, B., Bottazzi, M., Hadjidoukas, P., Fatichi, S., 2020. More green and less blue water in the Alps during warmer summers. Nat. Clim. Chang. 10, 155–161. https://doi.org/10.1038/s41558-019-0676-5.
McDowell, N., Pockman, W.T., Allen, C.D., Breshears, D.D., Cobb, N., Kolb, T., Plaut, J., Sperry, J., West, A., Williams, D.G., Yepez, E.A., 2008. Mechanisms of plant survival and mortality during drought: why do some plants survive while others succumb to drought? New Phytol. 178, 719–739. https://doi.org/10.1111/j.1469-8137.2008.02436.x.
Mencuccini, M., Manzoni, S., Christoffersen, B., 2019. Modelling water fluxes in plants: from tissues to biosphere. New Phytol. 222, 1207–1222. https://doi.org/10.1111/nph.15681.
Mencuccini, M., 2003. The ecological significance of long-distance water transport: short-term regulation, long-term acclimation and the hydraulic costs of stature across plant life forms. Plant Cell Environ. 26, 163–182.
Nagavciuc, V., Michel, S.L.L., Balting, D.F., Helle, G., Freund, M., Schleser, G.H., Steger, D.N., Lohmann, G., Ionita, M., 2023. A past and present perspective on the European summer vapour pressure deficit. Clim. Past Discuss. 2023, 1–29.
Novick, K.A., Miniat, C.F., Vose, J.M., 2016. Drought limitations to leaf-level gas exchange: results from a model linking stomatal optimization and cohesion–tension theory. Plant Cell Environ. 39, 583–596. https://doi.org/10.1111/pce.12657.
Oren, R., Sperry, J.S., Katul, G.G., Pataki, D.E., Ewers, B.E., Phillips, N., Schäfer, K.V.R., 1999. Survey and synthesis of intra- and interspecific variation in stomatal sensitivity to vapour pressure deficit. Plant Cell Environ. 22, 1515–1526. https://doi.org/10.1046/j.1365-3040.1999.00513.x.
Pappas, C., Matheny, A.M., Baltzer, J.L., Barr, A.G., Black, T.A., Bohrer, G., Detto, M., Maillet, J., Roy, A., Sonnentag, O., Stephens, J., 2018. Boreal tree hydrodynamics: asynchronous, diverging, yet complementary. Tree Physiol. 38, 953–964.
Peters, R.L., Fonti, P., Frank, D.C., Poyatos, R., Pappas, C., Kahmen, A., Carraro, V., Prendin, A.L., Schneider, L., Baltzer, J.L., Baron-Gafford, G.A., Dietrich, L., Heinrich, I., Minor, R.L., Sonnentag, O., Matheny, A.M., Wightman, M.G., Steppe, K., 2018. Quantification of uncertainties in conifer sap flow measured with the thermal dissipation method. New Phytol. 219, 1283–1299. https://doi.org/10.1111/nph.15241.
Peters, R.L., Speich, M., Pappas, C., Kahmen, A., von Arx, G., Graf Pannatier, E., Steppe, K., Treydte, K., Stritih, A., Fonti, P., 2019. Contrasting stomatal sensitivity to temperature and soil drought in mature alpine conifers. Plant Cell Environ. 42, 1674–1689. https://doi.org/10.1111/pce.13500.
Peters, R.L., Pappas, C., Hurley, A.G., Poyatos, R., Flo, V., Zweifel, R., Goossens, W., Steppe, K., 2021. Assimilate, process and analyse thermal dissipation sap flow data using the TREX r package. Methods Ecol. Evol. 12, 342–350. https://doi.org/10.1111/2041-210X.13524.
Peters, R.L., Steppe, K., Pappas, C., Zweifel, R., Babst, F., Dietrich, L., Arx, G., Poyatos, R., Fonti, M., Fonti, P., Grossiord, C., Gharun, M., Buchmann, N., Steger, D.N., Kahmen, A., 2023. Daytime stomatal regulation in mature temperate trees prioritizes stem rehydration at night. N Phytol 239, 533–546.
Phillips, N., Oren, R., 1998. A comparison of daily representations of canopy conductance based on two conditional time-averaging methods and the dependence of daily conductance on environmental factors. Annales des Sciences Forestiéres 55, 217–235.
Pickett S.T.A. (1989) Space-for-Time Substitution as an Alternative to Long-Term Studies BT - Long-Term Studies in Ecology: Approaches and Alternatives. In: Likens GE (ed) Springer New York, New York, NY, pp 110–135. https://doi.org/10.1007/978-1-4615-7358-6_5.
Poyatos, R., Martínez-Vilalta, J., Čermák, J., Ceulemans, R., Granier, A., Irvine, J., Köstner, B., Lagergren, F., Meiresonne, L., Nadezhdina, N., Zimmermann, R., Llorens, P., Mencuccini, M., 2007. Plasticity in hydraulic architecture of Scots pine across Eurasia. Oecologia 153, 245–259. https://doi.org/10.1007/s00442-007-0740-0.
R Core Team, 2019. R: A language and environment for statistical computing. R Foundation for Statistical Computing, Vienna, Austria. URL: https://www.R-project.org/.
RStudio Team, 2020. RStudio: Integrated Development for R. RStudio, PBC, Boston, MA URL http://www.rstudio.com/.
Salomón, R.L., Limousin, J., Ourcival, J., Rodríguez-Calcerrada, J., Steppe, K., 2017. Stem hydraulic capacitance decreases with drought stress: implications for modelling tree hydraulics in the Mediterranean oak Quercus ilex. Plant, Cell Environ. 40, 1379–1391. https://doi.org/10.1111/pce.12928.
Salomón, R.L., Peters, R.L., Zweifel, R., Sass-Klaassen, U.G.W., Stegehuis, A.I., Smiljanic, M., Poyatos, R., Babst, F., Cienciala, E., Fonti, P., Lerink, B.J.W., Lindner, M., Martinez-Vilalta, J., Mencuccini, M., Nabuurs, G.-J., van der Maaten, E., von Arx, G., Bär, A., Akhmetzyanov, L., Balanzategui, D., Bellan, M., Bendix, J., Berveiller, D., Blaženec, M., Čada, V., Carraro, V., Cecchini, S., Chan, T., Conedera, M., Delpierre, N., Delzon, S., Ditmarová, Ľ., Dolezal, J., Dufrêne, E., Edvardsson, J., Ehekircher, S., Forner, A., Frouz, J., Ganthaler, A., Gryc, V., Güney, A., Heinrich, I., Hentschel, R., Janda, P., Ježík, M., Kahle, H.-P., Knüsel, S., Krejza, J., Kuberski, Ł., Kučera, J., Lebourgeois, F., Mikoláš, M., Matula, R., Mayr, S., Oberhuber, W., Obojes, N., Osborne, B., Paljakka, T., Plichta, R., Rabbel, I., Rathgeber, C.B.K., Salmon, Y., Saunders, M., Scharnweber, T., Sitková, Z.,

Stangler, D.F., Stereńczak, K., Stojanović, M., Střelcová, K., Světlík, J., Svoboda, M., Tobin, B., Trotsiuk, V., Urban, J., Valladares, F., Vavrčík, H., Vejpustková, M., Walthert, L., Wilmking, M., Zin, E., Zou, J., Steppe, K., 2022. The 2018 European heatwave led to stem dehydration but not to consistent growth reductions in forests. Nat. Commun. 13, 28. https://doi.org/10.1038/s41467-021-27579-9.

Satoh, Y., Yoshimura, K., Pokhrel, Y., Kim, H., Shiogama, H., Yokohata, T., Hanasaki, N., Wada, Y., Burek, P., Byers, E., Schmied, H.M., Gerten, D., Ostberg, S., Gosling, S.N., Boulange, J.E.S., Oki, T., 2022. The timing of unprecedented hydrological drought under climate change. Nat. Commun. 13, 3287. https://doi.org/10.1038/s41467-022-30729-2.

Saxton, K.E., Rawls, W.J., 2006. Soil Water Characteristic Estimates by Texture and Organic Matter for Hydrologic Solutions. Soil Sci. Soc. Am. J. 70, 1569–1578. https://doi.org/10.2136/sssaj2005.0117.

Schönbeck, L., Grossiord, C., Gessler, A., Gisler, J., Meusburger, K., D'Odorico, P., Rigling, A., Salmon, Y., Stocker, B.D., Zweifel, R., Schaub, M., 2022. Photosynthetic acclimation and sensitivity to short- and long-term environmental changes in a drought-prone forest. J. Exp. Bot. 73, 2576–2588. https://doi.org/10.1093/jxb/erac033.

Schlesinger, W.H., Jasechko, S., 2014. Transpiration in the global water cycle. Agric. For. Meteorol. 189-190, 115–117. https://www.sciencedirect.com/science/article/pii/S0168192314000203.

Siegmund, J.F., Sanders, T.G.M., Heinrich, I., Maaten, E.V.D., Simard, S., Helle, G., Donner, R.V., 2016. Meteorological drivers of extremes in daily stem radius variations of beech, oak, and pine in Northeastern Germany: an event coincidence analysis. Front. Plant Sci. 7, 1–14.

Steppe, K., Lemeur, R., 2007. Effects of ring-porous and diffuse-porous stem wood anatomy on the hydraulic parameters used in a water flow and storage model. Tree Physiol. 27, 43–52. https://doi.org/10.1093/treephys/27.1.43.

Steppe, K., Pauw, D.J.W.D., Lemeur, R., Vanrolleghem, P.A., 2006. A mathematical model linking tree sap flow dynamics to daily stem diameter fluctuations and radial stem growth. Tree Physiol. 26, 257–273. https://doi.org/10.1093/treephys/26.3.257.

Steppe, K., 2018. The potential of the tree water potential. Tree Physiol. 38, 937–940. https://doi.org/10.1093/treephys/tpy064.

Teepe, R., Dilling, H., Beese, F., 2003. Estimating water retention curves of forest soils from soil texture and bulk density. J. Plant Nutr. Soil Sci. 166, 111–119.

Tomasella, M., Beikircher, B., Häberle, K.-H., Hesse, B., Kallenbach, C., Matyssek, R., Mayr, S., 2017. Acclimation of branch and leaf hydraulics in adult Fagus sylvatica and Picea abies in a forest through-fall exclusion experiment. Tree Physiol. 38, 198–211. https://doi.org/10.1093/treephys/tpx140.

Tyree, M.T., Zimmermann, M.H., 2002. Hydraulic architecture of whole plants and plant performance. In: Tyree, MT, Zimmermann, MH (Eds.), Xylem Structure and the Ascent of Sap. Springer Berlin Heidelberg, Berlin, Heidelberg, pp. 175–214. https://doi.org/10.1007/978-3-662-04931-0_6.

Verbeeck, H., Steppe, K., Nadezhdina, N., de Beeck, M.O., Deckmyn, G., Meiresonne, L., Lemeur, R., Čermák, J., Ceulemans, R., Janssens, I.A., 2007. Stored water use and transpiration in Scots pine: a modeling analysis with ANAFORE. Tree Physiol. 27, 1671–1685. https://doi.org/10.1093/treephys/27.12.1671.

Walthert, L., Ganthaler, A., Mayr, S., Saurer, M., Waldner, P., Walser, M., Zweifel, R., von Arx, G., 2021. From the comfort zone to crown dieback: sequence of physiological stress thresholds in mature European beech trees across progressive drought. Sci. Total Environ. 753, 141792. https://www.sciencedirect.com/science/article/pii/S0048969720353213.

Wu, C., Peng, J., Ciais, P., Peñuelas, J., Wang, H., Beguería, S., Andrew Black, T., Jassal, R.S., Zhang, X., Yuan, W., Liang, E., Wang, X., Hua, H., Liu, R., Ju, W., Fu, Y. H., Ge, Q., 2022. Increased drought effects on the phenology of autumn leaf senescence. Nat. Clim. Chang 12, 943–949. https://doi.org/10.1038/s41558-022-01464-9.

Zimmermann, J., Link, R.M., Hauck, M., Leuschner, C., Schuldt, B., 2021. 60-year record of stem xylem anatomy and related hydraulic modification under increased summer drought in ring- and diffuse-porous temperate broad-leaved tree species. Trees 35, 919–937. https://doi.org/10.1007/s00468-021-02090-2.

Zuur, A.F., Ieno, E.N., Elphick, C.S., 2010. A protoscol for data exploration to avoid common statistical problems. Methods Ecol. Evol. 1, 3–14. https://doi.org/10.1111/j.2041-210X.2009.00001.x.

Zweifel, R., Zimmermann, L., Newbery, D.M., 2005. Modeling tree water deficit from microclimate: an approach to quantifying drought stress. Tree Physiol. 25, 147–156. https://doi.org/10.1093/treephys/25.2.147.

Zweifel, R., Haeni, M., Buchmann, N., Eugster, W., 2016. Are trees able to grow in periods of stem shrinkage? New Phytol. 211, 839–849. https://doi.org/10.1111/nph.13995.